Chemical Engineering Journal 168 (2011) 413–419

Contents lists available at ScienceDirect

Chemical Engineering Journal

journal homepage: www.elsevier.com/locate/cej

Diesel particulate matter combustion with CeO_2 as catalyst. Part II: Kinetic and reaction mechanism

Martín S. Gross, Bárbara S. Sánchez, Carlos A. Querini*

Instituto de Investigaciones en Catálisis y Petroquímica (INCAPE) – FIQ – UNL – CONICET, Santiago del Estero 2654, Santa Fe S3000AOJ, Argentina

ARTICLE INFO

Article history:
Received 19 April 2010
Received in revised form 17 January 2011
Accepted 17 January 2011

Keywords:
Diesel particulate matter
Oxidation kinetics
Reaction mechanism
Cerium oxide

ABSTRACT

In this work, a reaction mechanism for the soot oxidation reaction on ceria is presented. The mechanism is based on kinetic and characterization results previously obtained. Temperature-programmed oxidation analyses using different heating rates, up to different final temperatures, as well as isothermal combustions, have been carried out to determine the kinetic behavior of this system. The reaction mechanism includes the formation of superoxides, peroxides, oxygen vacancies, surface diffusion, and the change of the type of contact between the carbon and the catalyst that occurs during the combustion. The kinetic parameters are obtained using a single temperature-programmed profile, obtained at 12 °C/min. With these parameters, it is possible to predict the kinetic response obtained in many different experimental conditions. Particularly, the reaction rate at constant temperature may or may not present a maximum as a function of time, depending upon the value of the temperature. The mechanism proposed explained these observations. The calcination temperature has an important effect on the activity of the catalyst. As this temperature is increased a better activity is observed, being this behavior associated to an easier formation of superoxides and peroxides upon high temperature calcination.

1. Introduction

It is well known that cerium oxide decreases the soot burn-off temperature [1], due to its redox properties [2]. The soot is burnt by oxygen that cerium oxide provides, and not by molecular oxygen present in the gas phase [3,4].

There are many works about the reaction mechanism of carbonaceous material combustion in non catalytic [5–11] or catalytic processes [1–4,6,11–18]. However, detailed kinetic studies are not reported in most of these publications. A reason for the lack of good kinetic models is that this system is quite complex, involving two solid phases and a gas phase. The solid phases are the catalyst and the soot, and the gas phase contains oxygen and reaction products such as carbon dioxide. These phases have to be in contact in order to make it possible the reaction. In several works, kinetic expressions that correspond to pseudo-homogeneous models, such as the power law model [7,11,16], have been used. In these cases, the apparent kinetics parameters were calculated. On the other hand, heterogeneous kinetic models have been analyzed by several authors [3,13–15,17], even though in these works the kinetic parameters for each reaction step were not reported.

In order to study this catalytic system at a laboratory level, different ways of mixing the soot with the catalyst have been used. The level of physical interaction between the soot and the catalyst determines the reaction rate. There are two main procedures to mix these solids. In one of them, both phases are mixed by hand-grinding in a mortar or with a ball mill. This procedure leads to what is called 'tight contact' mode [30,31]. The other procedure consists in shaking the soot and the catalyst in a vial [32] or mixing them with a spatula [31]. This leads to the 'loose' contact mode. In a real soot trap, the loose-contact mode takes place. Depending on the objective of the study, one of these procedures is selected. For example, if the goal is to compare intrinsic catalytic activities, the tight contact mode is used.

The objective of this work is to determine a heterogeneous kinetic model, with capacity to reproduce experimental kinetics results of soot catalytic combustion, and to predict the kinetic response obtained under different experimental conditions. A reaction mechanism is proposed based on kinetic and catalytic characterization results obtained by XPS, FTIR, and SEM analyses [19]. The model is also based on the contribution of other research groups [2,3,20]. Non-linear regression was carried out in order to find the kinetics parameters for each reaction step. The reaction mechanism proposed in this work makes it possible to simulate and predict the catalytic soot combustion rate in conditions completely different from those at which the parameters were obtained. Moreover, the kinetic model that we present in this contribution

* Corresponding author. Tel.: +54 342 4533858; fax: +54 342 4531068.
E-mail address: querini@fiq.unl.edu.ar (C.A. Querini).

1385-8947/$ – see front matter © 2011 Elsevier B.V. All rights reserved.
doi:10.1016/j.cej.2011.01.060

can predict very well experimental results that other models cannot reproduce. All the study was carried out using the tight-contact mode and, therefore, it is valid to simulate the intrinsic kinetics of this catalytic system. The model is valid for the fresh catalyst. Catalyst deactivation is not included, therefore the effects of variables such as sulphur and ash deposition are not considered.

2. Experimental

2.1. Soot, catalysts, and catalyst:soot mixtures preparation

Soot was obtained by burning commercial diesel fuel as described in [21]. The soot was collected from the recipient walls and then was dried in a stove at 120 °C for 24 h.

Commercial cerium (IV) oxide 99.9% (Aldrich) was used as catalyst, after calcination at 450 °C and 800 °C for 2 h, and will be represented as CeO_2^{450} and CeO_2^{800}.

In this work, catalysts and soot were mixed with a mass ratio of 20:1. To prepare these mixtures, the weighted solids were placed in a mortar and were mechanically mixed for 6 min, obtaining in this way a tight contact.

2.2. Catalysts activity

Catalytic activity was determined by temperature-programmed oxidation tests (TPO), carried out with the catalyst:soot mixtures prepared as above described. The amount of sample loaded into the cell was 10 mg. Different temperature programmes were used in the TPO experiments. A set of experiments was carried out using different heating rates, e.g. 4, 8, 12 and 16 °C/min. A second set, consisted in heating the sample at 12 °C/min until a given pre-selected temperature was reached, and then holding this temperature for a given time. Finally, another set of TPO analyses was carried out heating the sample under an inert gas (N_2) flow, until a given temperature was reached. At this moment the gas was switched to an O_2/N_2 mixture holding a constant temperature. In all cases, the gas flow rate and composition were 40 cm^3/min and 5%O_2 (N_2 to balance), respectively. The gases coming out of the reaction cell went through a methanation reactor where the CO and CO_2 were converted to CH_4 with 100% conversion [22]. This reactor operated at 400 °C, and was loaded with a nickel catalyst. Methane formed in this reactor was continuously monitored with a FID.

Using a heating rate of 12 °C/min, 5% O_2 composition in gas phase, 40 cm^3/min gas flow rate and 10 mg of catalyst:soot mass (with a ratio 20:1) kinetic control is guaranteed, as was demonstrated in a previous work [23].

3. Model formulation

In the part I of this work [19], the mechanism proposed for catalytic diesel soot combustion on ceria was:

$$n\mathrm{CeO}_x + \mathrm{O}_2 \rightarrow [n\mathrm{CeO}_x]^+\mathrm{O}_2^- \quad (1)$$

$$[n\mathrm{CeO}_x]^+\mathrm{O}_2^- \leftrightarrow [n\mathrm{CeO}_x]^{2+}\mathrm{O}_2^{2-} \quad (2)$$

$$[n\mathrm{CeO}_x]^+\mathrm{O}_2^- \leftrightarrow n\mathrm{CeO}_y \quad (3)$$

$$[n\mathrm{CeO}_x]^{2+}\mathrm{O}_2^{2-} + \mathrm{C} \rightarrow [n\mathrm{CeO}_x]^{2+}[\mathrm{CO}_2]^{2-} \quad (4)$$

$$[n\mathrm{CeO}_x]^{2+}[\mathrm{CO}_2]^{2-} \rightarrow [n\mathrm{CeO}_x]^{2+}[\,]^{2-} + \mathrm{CO}_2 \quad (5)$$

$$[n\mathrm{CeO}_x]^{2+}[\,]^{2-} \rightarrow n\mathrm{CeO}_x \quad (6)$$

This is the 'rigorous' mechanism. Some simplifications can be introduced in the model taking into account the relative rates of each step.

The first simplification is to consider that peroxides ions do not form superoxides ions (reverse of reaction (2)). This is because the peroxides are the active oxygen species that react with soot (reaction (4)) and it is supposed that this reaction is faster than the reaction that yields superoxides. This is in agreement with the proposal of Bueno-López et al. [3]. In this work the authors concluded that the rate of active oxygen reaction with soot is much faster than the rate of its combination giving gaseous molecular oxygen. Therefore the reaction (2) can be rewritten as an irreversible step:

$$[n\mathrm{CeO}_x]^+\mathrm{O}_2^- \rightarrow [n\mathrm{CeO}_x]^{2+}\mathrm{O}_2^{2-} \quad (7)$$

Based on this assumption, i.e. that the peroxides are mainly consumed during soot combustion (reaction (4)), it can also be assumed that reaction (3) will not proceed to any significant extent.

Another simplification is to consider that the steps that describe carbon dioxide desorption (reaction (5)) and the oxygen vacancy migration (reaction (6)) are fast enough, and, therefore, reactions (4)–(6) can be replaced by the following overall reaction:

$$[n\mathrm{CeO}_x]^{2+}\mathrm{O}_2^{2-} + \mathrm{C} \rightarrow n\mathrm{CeO}_x + \mathrm{CO}_2 \quad (8)$$

In this way, the reactions (1), (7) and (8) described the 'simplified' mechanism.

In the catalyst:soot mixture, not all the carbon atoms are in contact with the catalyst, therefore it has to be considered the combustion of carbon atoms that are not in the interface catalyst:soot:

$$[n\mathrm{CeO}_x]^{2+}\mathrm{O}_2^{2-} + \mathrm{C}^* \rightarrow n\mathrm{CeO}_x + \mathrm{CO}_2 \quad (9)$$

Where C* represents the carbon atoms that are in the interface soot:gas, and those represented by C are the carbon atoms that are in the interface catalyst:soot. This consideration has been done taking into account the works of Ciambelli et al. [20] and Krishna et al. [2]. Ciambelli et al. measured the carbon specific surface area at different conversion levels, providing evidence that the entire carbon surface participates in the reaction. Krishna et al. proposed that the active oxygen from the catalytic surface is able to reach the soot particles present as clusters (particles that are mostly in soot:gas interface) by spill-over.

During the reaction, as carbon conversion increases, those atoms that initially were not in contact with the catalyst, may change their position from the soot:gas interface, to the soot:catalyst interface, according to the reaction:

$$\mathrm{C}^* \rightarrow \mathrm{C} \quad (10)$$

This occurs not only due to the movement of the carbon, but also and mainly due to the movement of the active species of the catalyst.

The oxygen that reacts with both carbons species is the same. The difference is the way in which this oxygen reaches each type of carbon. The atoms that are in the catalyst:soot interface are reached by oxygen surface diffusion and the atoms that are in the soot:gas interface are reached by oxygen spillover.

The equations to be considered to model the kinetics of soot combustion in a fixed bed reactor, taking into account the reaction steps of the proposed mechanism, are the following:

$$\frac{\partial[n\mathrm{CeO}_x]}{\partial t} = -k_1\cdot[\mathrm{CeO}_x]\cdot P_{\mathrm{O}_2} + k_8\cdot[[\mathrm{CeO}_x]^{2+}\mathrm{O}_2^{2-}]\cdot[\mathrm{C}] + k_9\cdot[[\mathrm{CeO}_x]^{2+}\mathrm{O}_2^{2-}]\cdot[\mathrm{C}^*] \quad (11)$$

$$\frac{\partial[[n\mathrm{CeO}_x]^+\mathrm{O}_2^-]}{\partial t} = k_1\cdot[\mathrm{CeO}_x]\cdot P_{\mathrm{O}_2} - k_7\cdot[[\mathrm{CeO}_x]^+\mathrm{O}_2^-] \quad (12)$$

$$\frac{\partial[[n\mathrm{CeO}_x]^{2+}\mathrm{O}_2^{2-}]}{\partial t} = k_7\cdot[[\mathrm{CeO}_x]^+\mathrm{O}_2^-] - k_8\cdot[[\mathrm{CeO}_x]^{2+}\mathrm{O}_2^{2-}]\cdot[\mathrm{C}] - k_9\cdot[[\mathrm{CeO}_x]^{2+}\mathrm{O}_2^{2-}]\cdot[\mathrm{C}^*] \quad (13)$$

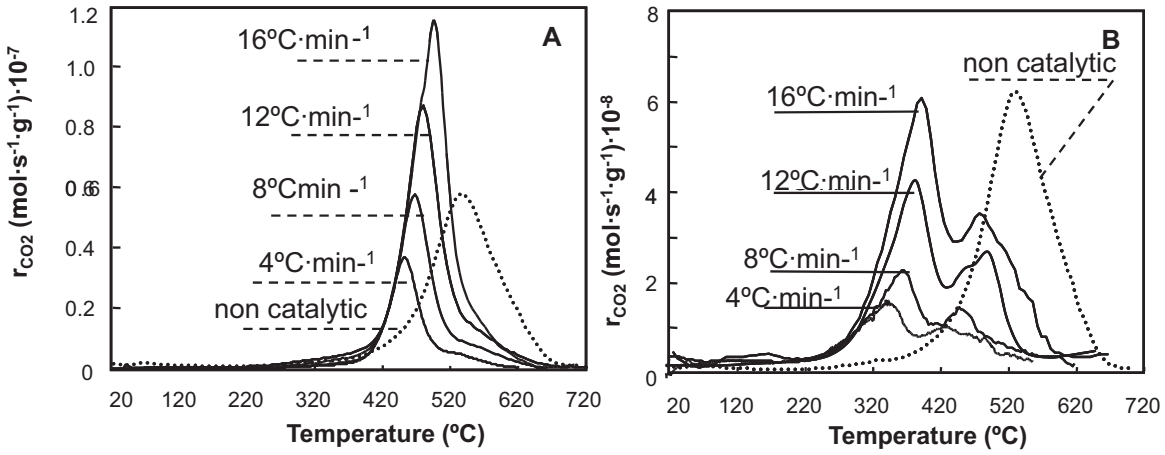

Fig. 1. Reaction rate *vs T* curves calculated from TPO experiments carried out at different heating rates. (A) CeO_2 calcined at 450 °C; (B) CeO_2 calcined at 800 °C.

$$\frac{\partial[C]}{\partial t} = -k_8 \cdot [[CeO_x]^{2+}O_2{}^{2-}] \cdot [C] + k_{10} \cdot [C^*] \quad (14)$$

$$\frac{\partial[C^*]}{\partial t} = -k_9 \cdot [[CeO_x]^{2+}O_2{}^{2-}] \cdot [C^*] - k_{10} \cdot [C^*] \quad (15)$$

$$F_{CO_2} = w_c \cdot \{k_8 \cdot [[CeO_x]^{2+}O_2{}^{2-}] \cdot [C] + k_9 \cdot [[CeO_x]^{2+}O_2{}^{2-}] \cdot [C^*]\} \quad (16)$$

The total amount of soot can be determined from the TPO profile, and represents the soot initial concentration (C_{ini}). Since we are assuming that this amount corresponds to soot in two different positions, the following mass balance must be taken into account:

$$C_{ini} = C_0 + C_0^* \quad (17)$$

The kinetic rate constant is designed as k_i, where the sub-index *i* corresponds to the number of the reaction in the above described mechanism. The concentration of each species in the set of equations (11)–(17) is given in mol/g, w_c (g) is the mass of catalyst loaded into the analysis cell, and F_{CO_2} (mol s^{-1}) the molar flow of CO_2 at the reactor outlet.

4. Results and discussion

4.1. Activity tests

Fig. 1 shows curves of reaction rate *vs* temperature for catalytic combustion at different heating rates. Results that correspond to catalyst calcined at 450 °C and 800 °C are shown in Fig. 1A and B, respectively. There are important differences in the activity between the oxides calcined at different temperatures. The catalyst calcined at low temperature displays the profile at a significantly higher temperature, and with a different shape. In addition, the maximum reaction rate reached with this catalyst is almost an order of magnitude higher than that obtained with the catalyst calcined at high temperature. Fig. 1B shows that the TPO profiles display two well-defined peaks, while in Fig. 1A the combustion profile reveals that there is a second peak at high-temperature, but it is included in the whole envelope. In Fig. 1 A and B, the non-catalytic combustion curve is included as reference. To obtain this curve, the soot was mixed with SiO_2 in the same proportion as with CeO_2. These results clearly indicate that the combustion of carbonaceous material is produced by the oxygen provided by ceria and not directly by molecular oxygen from the gas phase [19]. These different catalytic behaviors are due to the different surface compositions obtained at different calcination temperatures, as was previously shown [19]. It was found that at higher calcination temperature, the concentration of peroxides is higher [19]. In both cases, when the heating rate increases, the temperature at which the reaction rate reaches the maximum value is higher, and the peak height is higher. These results are in agreement with the predictions obtained using a simple power-law kinetic model [24]. Table 1 shows characteristic temperatures of the TPO profiles. These are: (i) TI, the temperature at which the soot combustion starts; (ii) TM, the temperature at which the reaction rate reaches the maximum value; (iii) TF, the temperature at which soot combustion finishes. It can be seen that TI and TM values are lower for the catalyst calcined at higher temperature. However, the TF values are similar in both catalysts.

The two peaks shown in the TPO profiles in Fig. 1B, can be related to the two types of carbon initially present on the system, as above proposed. These peaks are not well resolved in the case of the catalyst calcined at low temperature (Fig. 1A).

In order to obtain more and better information from temperature-programmed oxidation analysis, the final temperature has to be chosen at a level in such a way that only a fraction of the soot has been burnt [19–25]. Using this experimental design, we showed the different behaviors of the catalysts calcined at 450 °C and at 800 °C [19]. In the case of the former catalyst ($CeO_2{}^{450}$) the reaction rate keeps increasing as a function of time at constant temperature, depending upon the selected final value of temperature [19]. This phenomenon does not take place with the catalyst calcined at 800 °C ($CeO_2{}^{800}$). An example of this type of curve is shown in Fig. 3 (curve F).

4.2. Kinetic models for carbonaceous material combustion

Several kinetic models have been reported for carbon combustion reaction. Most of them correspond to the following expression:

$$r = A \cdot \exp\left(-\frac{E}{R \cdot T}\right) \cdot S \cdot P_{O_2}^m \quad (18)$$

Table 1
Characteristic temperatures of TPO showed in Fig. 1.

Heating rate	Calcined at 450 °C			Calcined at 800 °C		
	TI (°C)	TM (°C)	TF (°C)	TI (°C)	TM[a] (°C)	TF (°C)
4 °C/min	280	420	570	230	340	550
8 °C/min	280	450	630	230	360	580
12 °C/min	280	480	670	230	380	550
16 °C/min	280	490	640	230	390	590

[a]Corresponds to the first peak.

Table 2
Kinetic models for carbonaceous material combustion.

Model	$S(X)$	Reference
Power-law (grain)	$(1-X)^n$	[26]
Pore tree	$(1-X)\sqrt{(X/\varepsilon_0)+(1-X)}$	[27]
Random pore	$(1-X)\sqrt{1-\varphi\ln(1-X)}$	[5]
Random capillary	$(1-X)\sqrt{1-(B_0/2\pi B_1^2)\ln(1-X)}$	[28]
Bifurcated pore	$(1-X)\sqrt{1-(1/(\ln(1/(1-\varepsilon_{\text{micropore},0}))))\ln(1-X)}$	[29]

n: carbon reaction order, related to carbon morphology (shape/size); ε_0: initial porosity; φ: structure parameter; B_0: total pore length; B_1: total pore surface; $\varepsilon_{\text{micropore},0}$: initial micropore porosity.

where 'r' is the reaction rate, 'A' is the pre-exponential factor, 'E' is the activation energy, 'R' is the gases universal constant, 'T' is the absolute temperature, 'S' is the carbon surface exposed to reaction, 'P_{O_2}' is the oxygen partial pressure and 'm' is the oxygen reaction order. Table 2 shows well-known models for this reaction.

Fig. 2 shows simulations carried out using the models presented in Table 2. It can be seen that with random pore, random capillary and bifurcated pore models the reaction rate decays abruptly once the maximum reaction rate has been reached. On the other hand, the TPO simulated using the power-law and pore tree models are more symmetrical, being very similar between them. Partial burnt test was simulated with the same parameters set used to do the simulations shown in Fig. 2. The results are shown in Fig. 3. We found that none of the models previously reported in the literature can reproduce the experimental results. This is because these models does not contemplate all the phenomena that are taking place on the catalytic surface during soot combustion.

4.3. Parameters estimation and simulation

It is assumed that the reaction rate constants follow the Arrhenius law:

$$k_i = A_i \cdot \exp\left(-\frac{E_i}{R \cdot T}\right) \tag{19}$$

The parameters (A_i, E_i, C_0 and C_0^*) were estimated by non-linear regression of TPO experimental data obtained at 12 °C/min. Fig. 4 shows the experimental and simulated data for cerium oxide calcined at 450 °C. It can be seen that the agreement is very good. The estimated parameters values are listed in Table 3.

This set of parameters was used to simulate the TPO profiles obtained under different experimental conditions. This is usually a very good test to determine the capacity of the model to predict the behavior of the system, and consequently to give credibility to the reaction mechanism in which the model is based. Therefore, simulations were carried out at different heating rates, and different types of experiments, such as partial burnt tests and isothermal combustions. Simulations done with heating rates of 4, 8 and 16 °C/min perfectly reproduced the experimental results (not shown). The simulated profiles start at the same temperature independently of the heating rate, while the maximum reaction rate temperature and its height decrease as the heating rate decreases.

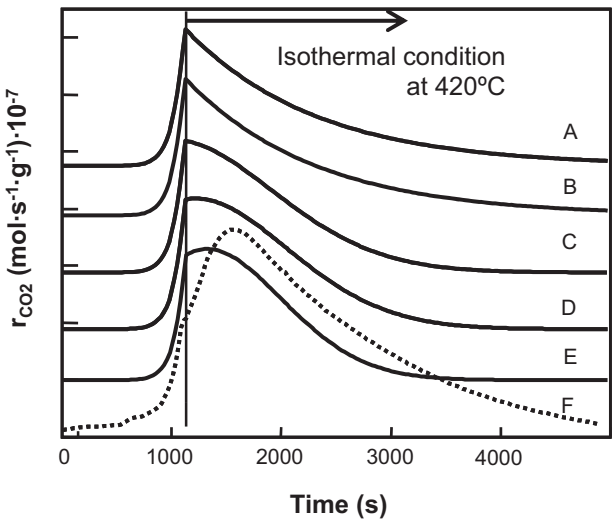

Fig. 3. Partial burnt test simulated with models listed in Table 2. (A) Power Law; (B) Pore Tree; (C) Random Pore; (D) Random Capillary; (E) Bifurcated Pore; (F) Experimental.

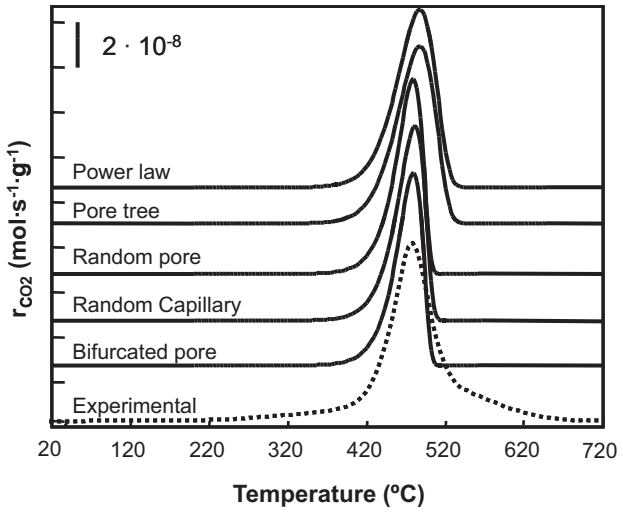

Fig. 2. TPO simulated with models listed in Table 2.

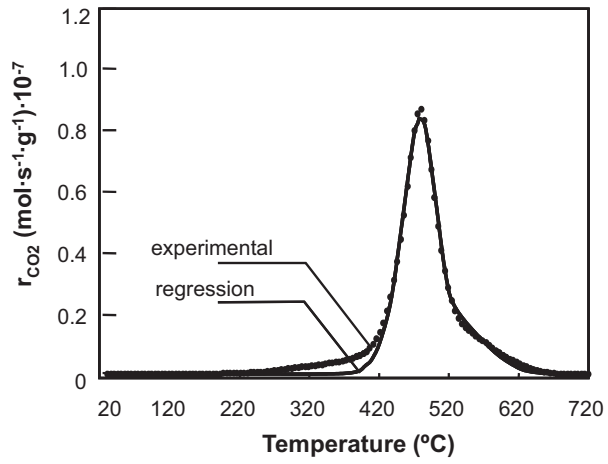

Fig. 4. Regression curve (full line) and experimental data (dotted line) for a TPO at 12 °C/min using CeO_2^{450} as catalyst.

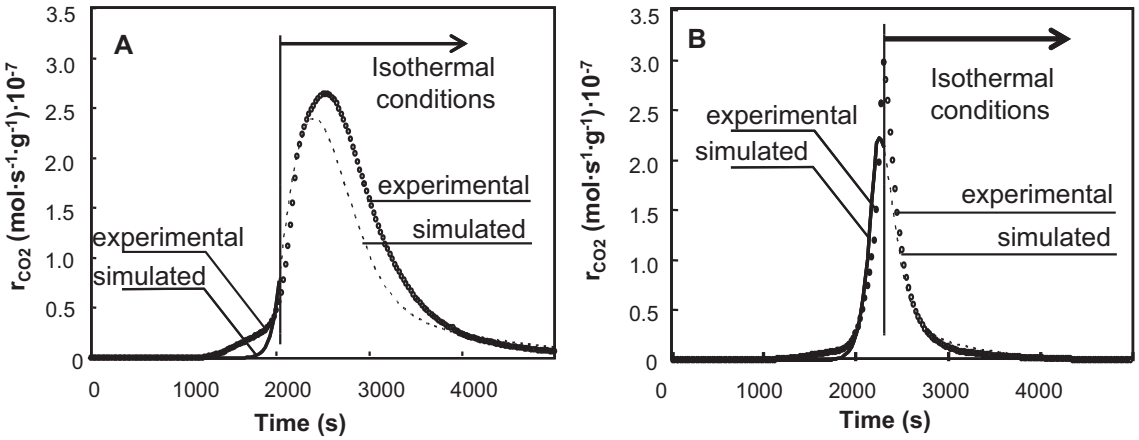

Fig. 5. Experimental and simulated data for partial burnt tests carried out at (A) 420 °C and (B) 460 °C using CeO_2^{450} as catalyst.

Fig. 5 shows results for partial burnt tests. As was shown in a previous work [19], at certain temperatures values, the reaction rate kept increasing under isothermal conditions. It can be seen in Fig. 5A that the model proposed can successfully reproduce this behavior when the temperature is 420 °C. Fig. 5B shows the results obtained in a similar experiment, but with a different final temperature, being in this case 460 °C. It can be seen that the profile is different from that shown in Fig. 5A. The reaction rate decays when the isothermal condition is reached. In spite of this different behavior at each temperature, the model correctly predicts the response of the system. Therefore, the proposed kinetic model is capable of reproducing the increase in reaction rate at those temperatures for which this phenomenon occurs. Results obtained for isothermal burnt simulations (not shown) showed that the predicted curve follows very well the experimental data. The agreement between the experimental results obtained in all these kinetic measurements, and the prediction of the model indicates that the proposed mechanism very well represents the system. It is very important to emphasize, that *the kinetic parameters were obtained using a single TPO profile, obtained at* 12 °C*/min, and with these parameters, it is possible to predict the complex kinetic behavior of this reacting system.*

With the kinetic model, it is possible to estimate the concentration of the reaction intermediate compounds. Fig. 6 shows the relative concentration of superoxides, peroxides and reduced ceria, as a function of the temperature. The experiment simulated in this figure corresponds to a TPO carried out at 12 °C/min. It can be seen that superoxides species ($CeO_x^+O_2^-$) start to develop around 225 °C and its concentration reach a maximum at 425 °C, temperature that is 55 °C below the temperature at which the highest reaction rate is registered (see Fig. 1A). On the other hand, the peroxides ($CeO_x^{2+}O_2^{2-}$) concentration profile begins to develop at 350 °C and at 560 °C all CeO_x sites are bounded to peroxide. These profiles are useful to understand the results shown in Fig. 5, in which it was observed that the reaction rate presents a maximum in the test carried out at 420 °C while in the test carried out at 460 °C the rate shows a continuous decrease. The results shown in Fig. 6 indicate that at 460 °C there is significant amount of peroxides, being approximately 40% of the total sites on the surface. The model predicts that at 420 °C the superoxides species are reaching the maximum concentration, and the peroxides begin to develop. Therefore, as the concentration of these intermediates increases, the reaction rate also increases and, consequently, the maximum rate at constant temperature is observed. When the final temperature is 460 °C, the maximum peroxides formation rate has already occurred, and therefore the maximum rate for soot combustion at 460 °C is not observed.

The same kinetic model was used to estimate the kinetics parameters for the catalyst calcined at 800 °C. The characterization results obtained with these two catalysts (CeO_2^{450} and CeO_2^{800}) indicated that the difference between them are only a change in the concentration of the surface oxygen species, as determined by FTIR and XPS and a change in morphology as determine by SEM [19].

The soot used and the contact mode between the catalysts and the soot are the same for both catalysts. We suppose that only the kinetics parameters related to the steps that yield superoxide and peroxide should be different. The combustions steps, and the conversion of one type of carbon in another, should be the same for the

Table 3
Estimated kinetic parameters values for CeO_2^{450} catalyst.

Parameter	Step	Estimated value
A_1 (s^{-1} atm^{-1})	Superoxide formation	3,475
E_1 (cal mol^{-1})		18,564
A_7 (s^{-1})	Peroxide formation	5,649
E_7 (cal mol^{-1})		19,199
A_8 (g mol^{-1} s^{-1})	C carbon combustion	4,145
E_8 (cal mol^{-1})		15,131
A_9 (g mol^{-1} s^{-1})	C* carbon combustion	3,001
E_9 (cal mol^{-1})		20,459
A_{10} (s^{-1})	C* to C conversion	3,351
E_{10} (cal mol^{-1})		21,428
C_0 (mol g^{-1})		9.29×10^{-4}
C_0^* (mol g^{-1})		1.94×10^{-3}

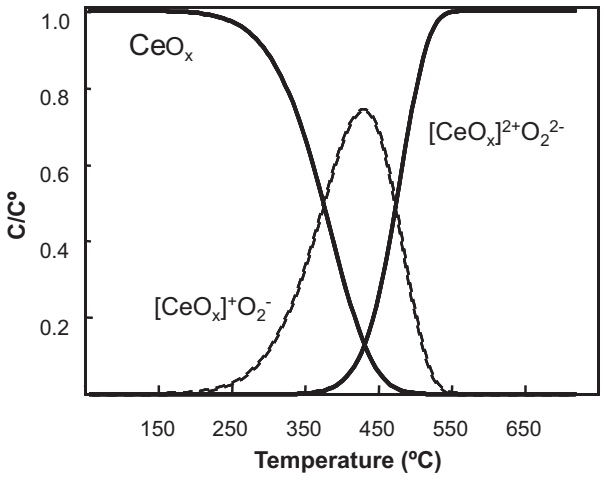

Fig. 6. Reaction intermediates relative concentration *vs T* for CeO_2^{450}.

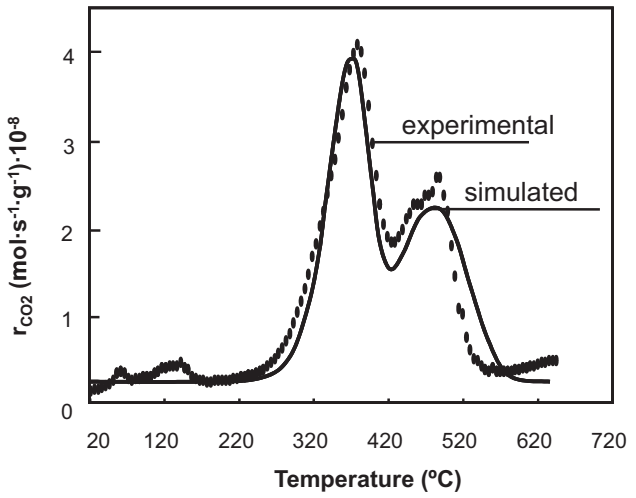

Fig. 7. Regression curve (full line) and experimental data (dotted line) for a TPO at 12 °C/min using CeO_2^{800} as catalyst.

oxide calcined at any temperature. Therefore, *the kinetic parameters that correspond to the combustions steps* (*reaction* (8) and (9)) *and the conversion of one carbon type in another* (*reaction* (10)), *are considered to be the same as those found with the catalyst calcined at* 450 °*C*.

Fig. 7 displays the regression curve and the experimental data that corresponds to a TPO carried out at 12 °C/min with the cerium oxide calcined at 800 °C. It can be seen that the regression is very good; it follows the complex combustion profile obtained with this catalyst. Table 4 shows the parameters values for cerium oxide calcined at 800 °C.

Comparing results for CeO_2^{450} (Table 3) and CeO_2^{800} (Table 4), it can be seen that the better activity of the catalyst calcined at higher temperature is due to changes in the rates of the steps that involve the superoxide and peroxide formation. In these steps, the pre-exponential factors are higher and the activation energies are lower when calcining the catalyst at high temperature.

Simulations carried out with the kinetic parameters given in Table 4 are shown in Figs. 8 and 9. For clarity reasons, Fig. 8 only displays the conversion *vs* temperature curves calculated from TPO profiles corresponding to heating rates of 8 and 16 °C/min. The model prediction capability is very good. Fig. 9 shows the experimental and simulated data of a partial combustion carried out with a final temperature of 340 °C. When the ceria is calcined at 800 °C, the same response is observed for all the values of final temperature studied, being similar to that shown in Fig. 9. As soon as the isothermal condition is reached, the reaction rate decays in an exponential way. It can be seen that the model follows the experimental results.

Fig. 10 displays the relative concentration of intermediate species *vs* temperature for cerium oxide calcined at 800 °C. The superoxide ion concentration is multiplied by a factor of 10^4 because the transformation rate of this specie in peroxides is very

Table 4
Estimated kinetic parameters values for CeO_2^{800} catalyst.

Parameter	Step	Estimated value
A_1^{**} (s^{-1} atm^{-1})	Superoxide formation	10,144
E_1^{**} (cal mol^{-1})		15,510
A_7^{**} (s^{-1})	Peroxide formation	12,009
E_7^{**} (cal mol^{-1})		8,313
A_8 (g mol^{-1} s^{-1})	C carbon combustion	4,145
E_8 (cal mol^{-1})		15,131
A_9 (g mol^{-1} s^{-1})	C* carbon combustion	3,001
E_9 (cal mol^{-1})		20,459
A_{10} (s^{-1})	C* to C conversion	3,351
E_{10} (cal mol^{-1})		21,428
C_0 (mol g^{-1})		1.51×10^{-3}
C_0^* (mol g^{-1})		1.48×10^{-3}

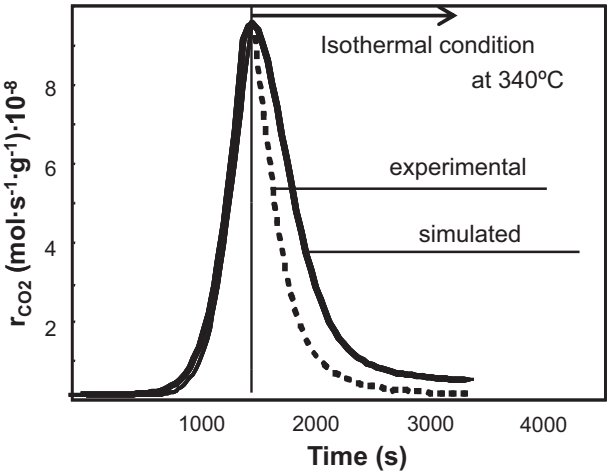

Fig. 9. Experimental and simulated data for partial burnt tests carried out at 340 °C. Catalyst: CeO_2^{800}.

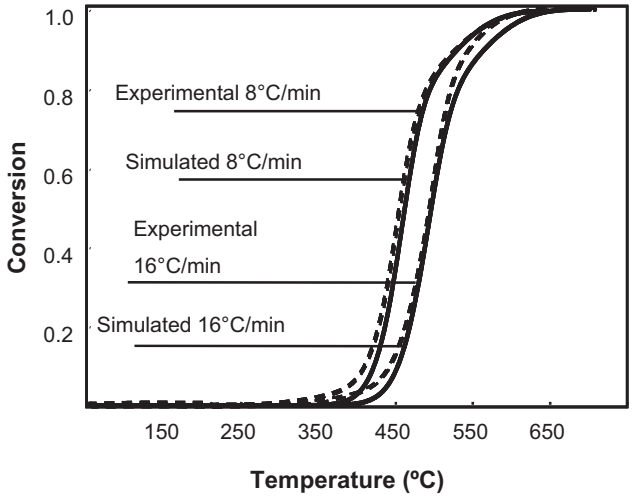

Fig. 8. Conversion *vs* Temperature curves, calculated from TPO experiments carried out at 8 and 16 °C/min. Catalyst: CeO_2^{800}.

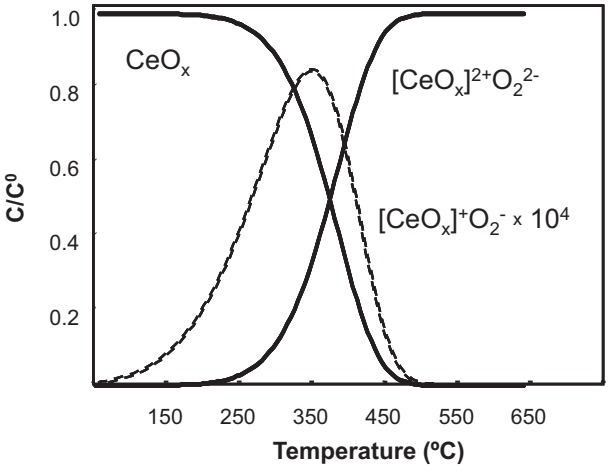

Fig. 10. Reaction intermediates relative concentration *vs T* for CeO_2^{800}.

high; therefore, the superoxide concentration reaches a maximum with a very small value. It can also be seen that at 500 °C the surface is completely covered by peroxides ions, while with the catalyst calcined at 450 °C a temperature of 560 °C was needed (Fig. 6). Another important difference is the temperature at which the maximum superoxides concentration is reached, being 425 °C for the catalyst calcined at 450 °C, and 350 °C for the catalyst calcined at 800 °C.

The characterization results previously reported [19] and the kinetic evidence presented in this work, suggest that the calcination at high temperature leads to a chemical structure that facilitates the formation of the superoxide and peroxide intermediates, and consequently the catalytic behavior is significantly modified.

The reaction mechanism proposed in this work is valid for a tight-contact mode between the soot and the catalyst. In order to simulate the operation of a real trap, this mechanism must be coupled with mass and energy transfer steps. Nevertheless, it is a difficult challenge to develop such complete model of this system. Another option is to find global kinetic parameters that can fit the kinetic response of the system under loose-contact mode. This latter case corresponds to an empirical model that might be useful for design purposes, but will not provide a detailed description of the reaction mechanism.

5. Conclusions

It has been found that when cerium oxide is calcined at high temperature, the catalyst has better activity for the soot oxidation reaction. The kinetic evidence indicates that this pretreatment leads to a structure that facilitates the formation of oxygenated surface or sub-surface compounds.

A kinetic model is proposed, being able to predict the catalytic soot combustion rate with ceria calcined at 450 °C or 800 °C. This model considers the superoxide and peroxide ions formation, being the latter the one that reacts with soot during combustion. When the peroxide ion reacts with soot, an oxygen vacancy is formed. Both, peroxides and oxygen vacancies have a high surface mobility. The surface diffusion processes are fast enough, not affecting the global reaction rate. The molecular oxygen enters into the metal oxide crystalline structure by interaction with the oxygen vacancies.

The proposed kinetic model considers two types of carbons. The first one, refers to the atoms that are in the catalyst:soot interface; and the second one refers to the carbon atoms that are in the soot:gas interface, i.e. the atoms that are in contact with gaseous phase. The peroxides reach the first type of carbons atoms by surface diffusion, while the second type of carbons are reached by spill-over.

Under certain isothermal conditions, the peroxide formation step in the cerium oxide calcined at 450 °C is the limiting rate step, causing that the reaction rate goes through a maximum. In the case of the ceria calcined at 800 °C, the formation of this intermediate is kinetically favored and occurs very fast, and consequently this behavior is not observed.

It has to be emphasized that the model can predict the kinetic response of the system using parameters estimated using only one TPO profile, what gives to the proposed mechanism more reliability.

References

[1] M.S. Gross, M.A. Ulla, C.A. Querini, Appl. Catal. A 360 (2009) 81–88.
[2] K. Krishna, A. Bueno-López, M. Makkee, J.A. Moulijn, Appl. Catal. B 75 (2007) 189–200.
[3] A. Bueno-López, K. Krishna, M. Makkee, J.A. Moulijn, J. Catal. 230 (2005) 237–248.
[4] A. Bueno-López, K. Krishna, B. van der Linden, G. Mul, J.A. Moulijn, M. Makkee, Catal. Today 121 (2007) 237–245.
[5] S.K. Bhatia, D.D. Perlmutter, AIChE J. 26 (1980) 379.
[6] G. Mul, J.P.A. Neeft, F. Kapteijn, J.A. Moulijn, Carbon 36 (1998) 1269–1276.
[7] A. Yezerets, N.W. Currier, D.H. Kim, H.A. Eadler, W.S. Epling, C.H.F. Peden, Appl. Catal. B 61 (2005) 120–129.
[8] W. Guo, H. Xiao, E. Yasuda, Y. Cheng, Carbon 44 (2006) 3269–3276.
[9] A. Messerer, R. Niessner, U. Pöschl, Carbon 44 (2006) 307–324.
[10] W. Guo, H. Xiao, Carbon 45 (2007) 1058–1065.
[11] P. Darcy, P. Da Costa, H. Mellottée, J.M. Trichard, G. Djéga-Mariadassou, Catal. Today 119 (2007) 252–256.
[12] J.P.A. Neeft, M. Makkee, J.A. Moulijn, Chem. Eng. J. 64 (1996) 295–302.
[13] M. Machida, Y. Murata, K. Kishikawa, D. Zhang, K. Ikeue, Chem. Mater. 20 (2008) 4489–4494.
[14] A. Trovarelli, M. Boaro, E. Rocchini, C. De Leitenburg, G. Dolcetti, J. Alloys Compd. 323–324 (2001) 584–591.
[15] L. Zhu, J. Yu, X. Wang, J. Hazard. Mater. 140 (2007) 205–210.
[16] M.N. Bokova, C. Decarne, E. Abi-Aad, A.N. Pryakhin, V.V. Lunin, A. Aboukaïs, Thermochim. Acta 428 (2005) 165–171.
[17] G. Mul, F. Kapteijn, C. Doornkamp, J.A. Moulijn, J. Catal. 179 (1998) 258–266.
[18] K. Shimizu, H. Kawachi, A. Satsuma, Appl. Catal. B 96 (2010) 169–175.
[19] M.S. Gross, M.A. Ulla, C.A. Querini, J. Mol. Catal., submitted for publication.
[20] P. Ciambelli, M. D'Amore, V. Palma, S. Vaccaro, Combust. Flame 99 (1994) 413–421.
[21] C.A. Querini, M.A. Ulla, F. Requejo, J. Soria, U.A. Sedrán, E.E. Miró, Appl. Catal. B 15 (1998) 5–19.
[22] S.C. Fung, C.A. Querini, J. Catal. 138 (1992) 240–254.
[23] M.A. Peralta, M.S. Gross, B.S. Sánchez, C.A. Querini, Chem. Eng. J. 152 (2009) 234–241.
[24] C.A. Querini, S.C. Fung, Appl. Catal. A 117 (1994) 53–74.
[25] B.S. Sánchez, M.S. Gross, B. Dalla Costa, C.A. Querini, Appl. Catal. A 364 (2009) 35–41.
[26] S.K. Bhatia, J.S. Gupta, Rev. Chem. Eng. 8 (1992) 177–258.
[27] G.A. Simons, M.L. Finson, Combust. Sci. Technol. 19 (1979) 217–255.
[28] G.R. Gavalas, AIChE J. 26 (1980) 577–585.
[29] H.P. Tseng, T.F. Edgar, Fuel 68 (1989) 114–119.
[30] S. Yuan, P. Mériaudeau, V. Perrichon, Appl. Catal. B: Environ. 3 (1994) 319.
[31] J.P.A. Neeft, O.P. van Pruissen, M. Makkee, J.A. Moulijn, Appl. Catal. B: Environ. 12 (1997) 21.
[32] R. Matarrese, L. Castoldi, L. Lietti, P. Forzatti, Catal. Today 136 (2008) 11.